

The application study of dual-energy CT nonlinear blending technique in pulmonary angiography*

Siqi Yi, Peng Zhou, Yakun He, Changjiu He, Shibe Hu (✉)

Department of Radiology, Sichuan Cancer Hospital & Institute, Sichuan Cancer Center, University of Electronic Science and Technology of China, Chengdu 610041, China

Abstract

Objective This study aimed to explore the feasibility of enhancing image quality in computed tomography (CT) pulmonary angiography (CTPA) and reducing radiation dose using the nonlinear blending (NLB) technique of dual-energy CT.

Methods A total of 61 patients scheduled for CTPA were enrolled, and 30 patients underwent dual-energy scanning. Nonlinear blending images (NLB group) and three groups of linear blending images (LB group, 80 kV group, and 140 kV group) were reconstructed after scanning; 31 patients underwent single-energy scanning (120 kV group). The CT values and standard deviations of the pulmonary trunk, left and right pulmonary arteries, and ipsilateral back muscle at the bifurcation level of the left and right pulmonary arteries were measured. The signal-to-noise ratio (SNR) and contrast-to-noise ratio (CNR) of the five groups were calculated. The subjective image quality of the five groups was assessed. The radiation doses of the dual- and single-energy groups were recorded and calculated.

Results The CNR and SNR values of blood vessels in the NLB group were significantly higher than those in the LB, 140 kV, and 80 kV groups (CNR of pulmonary artery trunk: $t = 3.50, 4.06, 7.17$, all $P < 0.05$; SNR of pulmonary trunk: $t = 3.76, 4.71, 6.92$, all $P < 0.05$). There were no statistical differences in the CNR and SNR values between the NLB group and 120 kV group ($P > 0.05$). The effective radiation dose of the dual-energy group was lower than that of the single-energy group ($t = -4.52, P < 0.05$). The subjective scores of images in the NLB group were the highest (4.28 ± 0.74).

Conclusion The NLB technique of dual-energy CT can improve the image quality of CTPA and reduce the radiation dose, providing more reliable imaging data for the clinical diagnosis of pulmonary embolism.

Key words: dual-energy computed tomography (CT); CT pulmonary angiography (CTPA); non-linear blending (NLB); image quality; radiation dose

Received: 18 December 2021
Revised: 14 October 2022
Accepted: 16 January 2023

Computed tomography pulmonary angiography (CTPA) is an accurate and reliable noninvasive imaging method for the diagnosis of pulmonary embolism (PE)^[1]. In this study, an intelligent tracking method of segmented injection of contrast agent is adopted, which can not only avoid the poor image quality caused by the difference in individual cycles when using the empirical value method but also reduce the radiation dose and contrast agent dosage by the low-dose test method. The image quality can also be improved using reconstruction technology^[2].

The non-linear blending (NLB) technique of dual-energy computed tomography (CT) can improve image quality by changing the calculation method of the CT

value, preserving the enhancement degree of blood vessels, and reducing soft tissue noise^[3]. The NLB technique has been used to improve the image quality of cranial vessels^[4-5], abdominal vessels^[6], and pulmonary nodules^[7]. However, there are few studies on the application of this technique to pulmonary arteries. Patients with PE often require multiple examinations with short intervals, and the quality of CTPA images is easily affected by circulatory differences in contrast agents in different individuals. Therefore, the study of NLB technology is of great clinical significance in improving the CTPA image quality and reducing the radiation dose.

✉ Correspondence to: Shibe Hu. Email: h13438823608@163.com

* Supported by a grant from the Science and Technology Plan of Sichuan Province (No. 2021YFS0225) and the Science and Technology Plan of Chengdu (No. 2021-YF05-01507-SN).

© 2023 Huazhong University of Science and Technology

Materials and methods

Clinical data

We enrolled 65 patients who were suspected of having PE or lung aspiration system-related diseases and underwent CTPA examination with dual-energy CT in our hospital (Sichuan Tumor Hospital, Chengdu, China) from July 2020 to March 2021. All patients signed an informed consent form before participating. Patients were considered ineligible for the study if they had a history of an iodine allergy reaction, cardiac or renal failure (glomerular filtration rate < 30 mL/min), untreated hyperthyroidism, or are pregnant or lactating. Four patients were excluded after examination because of inability to hold their breath or have poor breath holding. Finally, 61 cases were included in the study and randomly divided into experimental and control groups. Dual-energy scanning was performed in the experimental group, including 14 males and 16 females [mean age (51.7 ± 10.2) years old, 31–72 years old; mean body mass index (BMI) (23.0 ± 2.7) kg/m², range 19.10–27.34 kg/m²]. There were 19 males and 11 females in the control group (mean age (55.5 ± 7.4) years, 43–75 years old; mean BMI (23.1 ± 2.9) kg/m², range 18.11–26.67 kg/m²).

Instruments and methods

CT scanning protocol

All CT scans were acquired using a second-generation dual-energy CT device (Somatom Definition Flash, Siemens Healthcare, Forchheim, Germany), using automatic tube current; a pitch of 1.2; 128 × 0.66-mm collimator width; 0.28-msec tube rotation time; and 350 mm × 350 mm visual field of view (FOV). The voltage of the single-energy tube was 120 kV and the dual-energy was 80/Sn140 kVp.

All patients were positioned supine, with their feet on the scanning table. After acquiring the scout radiograph, the monitoring layer was placed in the right ventricle. A scan was triggered automatically when the CT threshold reached 50 HU after a 5-msec fixed delay with the contrast agent intelligent tracking technology and real-time dynamic exposure dose adjustment CARE Dose 4D technology. Each research was obtained after the participant was instructed to hold his or her breath following inhalation.

Injection scheme

CT images were taken after a 25-mL non-ionic contrast agent (370 mg/mL iodine) was administered through the right antecubital venous catheter at a flow rate of 5 mL/s or 4 mL/s. The injection rate was based on the patency of the patient's blood vessels using a dual-syringe injector. First, 20-mL saline was injected, followed by a combination of 30% contrast agent and 70% saline in 20-mL volume, and finally 30 mL of saline flushing^[8–9].

Image postprocessing and grouping

All image data were transmitted to the image workstation of the CT equipment (Syngo Via VB20, Siemens Healthcare) for postprocessing. After the experimental group acquired the dual-energy mode, four different series of images were reconstructed: 80 kV images, 140 kV images, LB images, and NLB images. NLB images were obtained by nonlinear blending with the equipment's own postprocessing Optimum Contrast software. The control group used single-energy scanning mode to obtain and reconstruct the 120-kV images.

When LB images are reconstructed with a default linear blending ratio of 0.6, the low-kVp information is multiplied by 0.6 and added to the high-kVp component, which is multiplied by 0.4. Unlike the LB technology, which uses a constant weighted contribution, the NLB algorithm establishes a smooth transition area that gradually increases the weighted contribution of the low-kVp image from 60% to 100% as a function of the CT number. The blending width (BW) is defined as the extent of the transition zone for image blending, and the blending center (BC) is defined as the center of the BW relative to the full CT number scale. In this study, BW was set at 200 and BC was at 150^[10].

After each scan, the dose-length product (DLP) and volume CT dose index (CTDI_{vol}) were recorded according to the patient protocol. The individual effective radiation dose (ED) was calculated using DLP values and a suitable standard conversion factor. $ED = K \times DLP$ ($K = 0.059$).

Image quality analysis

Qualitative analysis

After all images were processed, the subjective image quality was evaluated by two radiologists with more than 5 years of working experience. The experimental group images (NLB, LB, 80 kV, and 140 kV) and the control group images (120 kV) were displayed side-by-side, and the readers were blinded to the reconstruction methods. The 5-point scale method was adopted, and the specific scoring criteria are listed in Table 1^[11]. The readers were allowed to change their windows or level settings according to their personal preferences.

Quantitative analysis

Image contrast was evaluated using region of interest (ROI) measurements to calculate the contrast-to-noise ratio (CNR) and signal-to-noise ratio (SNR) values. Four ROIs were placed in the left, right, and trunk of pulmonary arteries, as well as the ipsilateral dorsal muscles, to measure CT values and standard deviation (SD) at the bifurcation level of left and right pulmonary arteries. The SD values of the ipsilateral muscles were used to represent background noise.^[11] SNR and CNR of the three consecutive layers were calculated as follows: $SNR = HU_{vessel} / StdDev_{muscle}$, $CNR = (HU_{vessel} - HU_{muscle}) /$

Table 1 The subjective evaluation criterion for image quality

Scores	The evaluation criterion
5	The pulmonary artery and its branches are shown clearly, and there is no obvious background noise.
4	The pulmonary aorta and its branches are shown clearly, and the background noise is slight.
3	The pulmonary aorta and its branches are shown clearly, and the background noise is obvious.
2	The pulmonary artery and its branches are shown clearly, and there is too much background noise.
1	The CT value at the beginning of pulmonary aorta is less than 150 HU, or the vascular branches are blurred and the background noise is large.

StdDev_{muscle}.

Furthermore, the ROI should be paced in the position of the distal 1 cm at the bifurcation of the blood vessels to avoid areas with severe calcification or vascular stenosis and should be kept consistent in size, shape, and location using a copy-and-paste function^[12].

CTDI_{vol}, DLP, and ED values were compared between the experimental and control groups. The percentage dose reduction between these protocols was also calculated.

Statistical analysis

All statistical analyses were performed using SPSS 25.0 software. Results were presented as mean ± SD ($\bar{x} \pm s$) for parametric data. After logarithmic transformation, the CNR and SNR values of each group of images accorded with normal distribution and the variance was uniform. The values of ln(CNR) and ln(SNR) of five groups were analyzed using single-factor analysis of variance. If the difference was statistically significant, the least significant difference method was used to compare the mean of the samples. Comparison of ED, CTDI_{vol}, and DLP values between the dual-energy scan and single-energy scan was performed using independent-sample *t*-test. The Mann-Whitney *U* test was used for the subjective score of

dual-energy and single-energy scanning. Inter-observer agreement of subjective image analysis was assessed using Cohen’s kappa (values of 0–0.20, 0.21–0.40, 0.41–0.60, 0.61–0.80, and 0.81–1.00 represent slight, fair, moderate, substantial, and almost perfect agreement, respectively). A *P*-value of less than 0.05 was considered statistically significant.

Results

Image quality

Subjective image quality

Substantial agreement was found between the two readers for subjective image quality scores (kappa = 0.79). The NLB group had the highest score (mean point: 4.28 ± 0.74, range: 3–5, H = 215.724, *P* < 0.05). The scores of the five group images are shown in Table 2, and Fig. 1 depicts the pulmonary artery images of the two patients. As shown in Fig. 2, the CNR and SNR values of the NLB group at the pulmonary trunk were the highest in all images (10.69 and 12.00, respectively). The image contrast at the embolus was 296 HU in the 80-kV group, followed by the NLB group, 120-kV group, LB group, and 140-kV group, while the background noise in the 80-kV

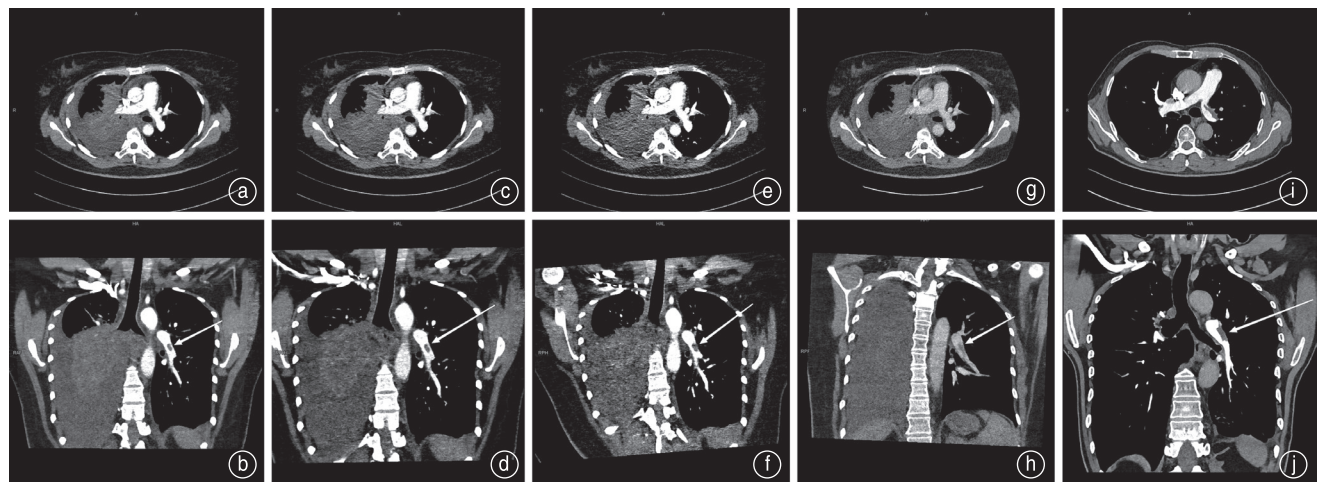


Fig. 1 (a–h) A 43-year-old woman with pulmonary embolism of the left lung artery segment and massive pleural effusion in right lung underwent dual-energy scanning with 80/Sn140 kVp. (i–j) A 63-year-old man with PE of the left lung artery trunk segment was scheduled to undergo single-energy scanning with 120 kV. NLB images are (a) and (b); LB images are (c) and (d); 80-kV images are (e) and (f); 140 kV images are (g) and (h); and 120kV images are (i) and (j). Pulmonary embolisms were demonstrated by the arrow in the images.

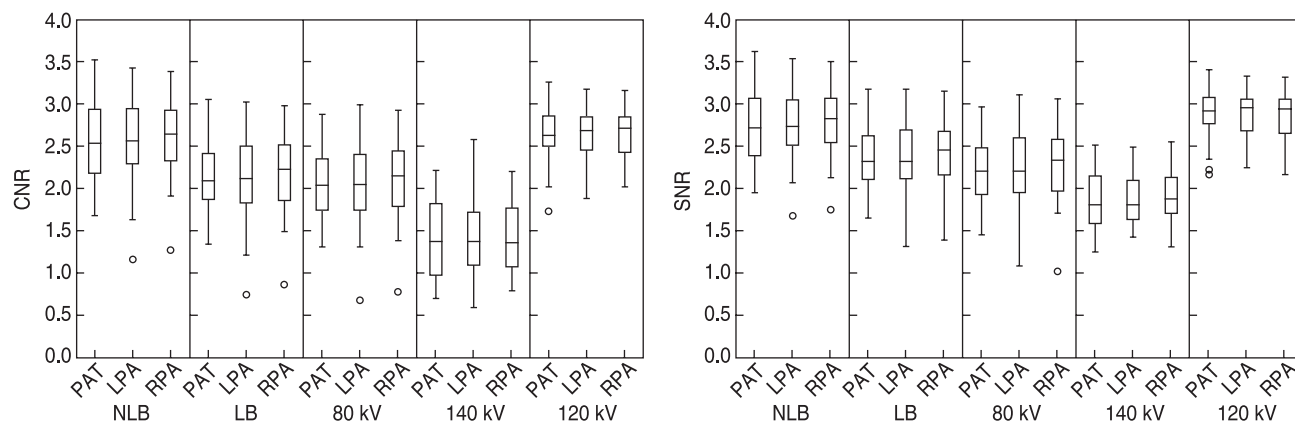


Fig. 2 Box-and-whisker plots show the median, interquartile spacing, and discrete values of CNR and SNR at the bifurcation level of the pulmonary artery at the pulmonary artery trunk (PAT), left pulmonary artery trunk (LPA), and right pulmonary artery trunk (RPA) in five sets of images.

Table 2 Comparisons of $\ln(\text{CNR})$, $\ln(\text{SNR})$ and subjective image qualities between five groups ($\bar{x} \pm s$)

Groups	Pulmonary trunk		Left pulmonary artery		Right pulmonary artery		The score of image quality
	$\ln(\text{CNR})$	$\ln(\text{SNR})$	$\ln(\text{CNR})$	$\ln(\text{SNR})$	$\ln(\text{CNR})$	$\ln(\text{SNR})$	
NLB	2.56 ± 0.50	2.74 ± 0.43	2.58 ± 0.51	2.78 ± 0.42	2.60 ± 0.48	2.79 ± 0.41	4.28 ± 0.74
LB	2.13 ± 0.43	2.36 ± 0.37	2.12 ± 0.50	2.36 ± 0.42	2.18 ± 0.46	2.41 ± 0.39	3.67 ± 0.82
80 kV	2.05 ± 0.42	2.22 ± 0.36	2.05 ± 0.50	2.23 ± 0.44	2.11 ± 0.47	2.27 ± 0.43	3.74 ± 0.50
140 kV	1.41 ± 0.48	1.87 ± 0.37	1.37 ± 0.57	1.87 ± 0.30	1.40 ± 0.43	1.88 ± 0.31	1.47 ± 0.50
120 kV	2.65 ± 0.35	2.89 ± 0.30	2.64 ± 0.34	2.87 ± 0.30	2.63 ± 0.33	2.86 ± 0.29	3.89 ± 0.75
F/H value	37.902	36.2338	32.600	34.860	38.919	34.796	215.724
P value	< 0.001	< 0.001	< 0.001	< 0.001	< 0.001	< 0.001	< 0.001

Table 3 Radiation dose evaluation index of dual-energy and single-energy scanning ($\bar{x} \pm s$)

	Dual-energy	Single-energy	<i>t</i>	<i>P</i>
ED (mSv)	1.16 ± 0.14	1.43 ± 0.29	-4.529	0.002
DLP (mGy/cm)	198.63 ± 23.78	243.71 ± 48.99	-4.484	0.002
CTDI _{vol} (mGy)	5.15 ± 0.60	7.15 ± 1.62	-6.249	< 0.001

group was the highest, followed by the LB group, the 120-kV group, NLB group, and the 140-kV group. Finally, the NLB group displayed better blood vessels and emboli than the other groups.

Objective image quality

There were significant differences in $\ln(\text{CNR})$ and $\ln(\text{SNR})$ among the five groups ($P < 0.05$; Table 2 and Fig. 2). The values of CNR and SNR in the NLB group were both higher than those in the LB, 140-kV, and 80-kV groups [CNR of the NLB group vs. LB group: pulmonary artery trunk (PAT), left pulmonary artery trunk (LPA), and right pulmonary artery trunk (RPA), $t = 3.50, 3.58,$ and 3.61 , all $P < 0.05$; 140-kV group: PAT, LPA, and RPA, $t = 4.06, 4.09,$ and 4.14 , all $P < 0.05$; 80-kV group: PAT, LPA, and RPA, $t = 7.17, 7.60,$ and 8.29 , all $P < 0.05$. SNR of the NLB group vs. LB group: PAT, LPA, and RPA, $t = 3.76, 3.68,$ and 3.74 , all $P < 0.05$; 140-kV group: PAT,

LPA, and RPA, $t = 4.71, 4.70,$ and 4.82 , all $P < 0.05$; 80-kV group: PAT, LPA, and RPA, $t = 6.92, 7.74,$ and 8.07 , all $P < 0.05$]. There were no significant differences in CNR and SNR between the NLB and 120-kV groups (CNR of the NLB group vs. LB group: PAT, LPA, and RPA, $t = -0.38, 0.01,$ and 0.195 , $P = 0.707, 0.992,$ and 0.846 , respectively). SNR of the NLB group vs. LB group: PAT, LPA, and RPA, $t = -1.003, -0.612,$ and -0.395 , $P = 0.320, 0.543,$ and 0.694 , respectively).

Radiation dosage

There were significant differences in the CTDI_{vol}, DLP, and ED between dual-energy and single-energy scanning (CTDI_{vol}: $t = -6.249$; DLP: $t = -4.484$; ED: $t = -4.529$; $P < 0.05$). Compared with the single-energy group, the values of CTDI_{vol}, DLP, and ED in the dual-energy group decreased by 30.0%, 18.5%, and 19.9%, respectively (Table 3).

Discussion

We evaluated the potential value of nonlinear blending postprocessing algorithm for improving the contrast resolution of CTPA images and reducing the radiation dose. A higher detection rate of PE was associated with

better SNR and CNR values in CT images. The results show that NLB technology can significantly improve the objective image quality of pulmonary artery CT images in dual-energy, and the image quality can be consistent with that of conventional single-energy scanning ($P > 0.05$). The subjective image quality score was the highest in the NLB group. Therefore, NLB technology can also be used to remedy the poor image quality of the pulmonary artery. In addition, the CTDI_{vol}, DLP, and ED values of the dual-energy group were lower than those of the single-energy group ($P < 0.05$), and there was a definite 19.9% decrease in the ED radiation dose in the dual-energy group. Compared with conventional 120-kV scanning, dual-energy NLB technology can reduce the radiation dose to ensure image quality.

Because CTPA has become the first choice for the diagnosis of PE, better and more reliable image quality is required. The pulmonary circulation time was very short (approximately 2–4 s). Early scanning of the distal pulmonary artery branch did not show adequate filling of the contrast agent, while the ray beam sclerosis artifact formed by the contrast agent in the superior vena cava and right ventricle will interfere with the display of emboli in the large pulmonary artery branch. When the scan is triggered too late, the contrast agent will fully fill the pulmonary vein, affecting the display of the segmental and subsegmental branches. Owing to these CTPA features, we used an intelligent tracking method to determine the most appropriate triggering time and found a suitable postprocessing method, NLB technology, to improve image quality.

Dual-energy CT collects high-kVp and low-kVp images in a single scan, with the low-kVp images increasing the CT value of the intravascular iodine contrast agent owing to the photoelectric effect and K-edge effect, which is useful for detecting emboli in pulmonary veins but has a high background noise. The noise of the high-kVp image is small, but due to the low intravascular CT value, the contrast between the blood vessel and the focus is poor, and the focus is easy to miss^[3]. Dual-energy CT image blending technology is divided into LB and NLB. The LB fuses high and low energies according to a fixed linear ratio. NLB is integrated according to the best proportion, using low-kVp images to reconstruct pixels with high CT values and high-kVp images to reconstruct pixels with low CT values, which not only retains high iodine contrast, but also reduces noise in a set of fused images^[3]. Among the many NLB methods, the most commonly used method (Moidal) is an improved S-shaped function curve fusion technique, which includes two parameters: BC and BW. The setting of different fusion parameters affects the image fusion. The BC value should be lower than the CT value of the blood vessel and higher than the CT value of the soft tissue around the blood vessel^[14].

Conventional scanning methods place the monitoring layer on the trunk of the pulmonary artery, ascending aorta, or descending aorta, and a 90-mL contrast agent is used. This study used a 25-mL contrast agent and placed the monitoring layer on the right ventricle at the pulmonary artery entrance. Whether this study can improve the success rate and repeatability of scanning and has the same diagnostic value is worthy of further study and discussion.

This study has some limitations. First, there were few experimental participants. Second, only the large pulmonary vessels were highlighted; however, clinically, most PEs are likely to occur in the twigs of the pulmonary arteries. Finally, diagnostic accuracy was not compared.

In summary, the NLB technique of dual-energy CT can improve the contrast of the pulmonary arteries, improve the image quality, and minimize the radiation dose, which is worthy of clinical application in practice.

Acknowledgments

Not applicable.

Funding

Supported by a grant from the Science and Technology Plan of Sichuan Province (No. 2021YFS0225) and the Science and Technology Plan of Chengdu (No. 2021-YF05-01507-SN).

Conflicts of interest

The authors declare no conflict of interest.

Author contributions

All authors contributed to data acquisition and interpretation, and have reviewed and approved the final version of this manuscript.

Data availability statement

Not applicable.

Ethical approval

Not applicable.

References

1. Abdellatif W, Ebada MA, Alkanj S, et al. Diagnostic accuracy of dual-energy CT in detection of acute pulmonary embolism: A systematic review and meta-analysis. *Can Assoc Radiol J.* 2021;72(2):285-292.
2. Konstantinides SV, Meyer G, Becattini C, et al. 2019 ESC Guidelines for the diagnosis and management of acute pulmonary embolism developed in collaboration with the European Respiratory Society (ERS). *Eur Heart J.* 2020;41(4):543-603.
3. De Santis D, Eid M, De Cecco CN, et al. Dual-energy computed tomography in cardiothoracic vascular imaging. *Radiol Clin North Am.* 2018;56(4):521-534.
4. Wang GS, Lyu FJ, Zhou Y, et al. Value of non-linear blending

- technique in head and neck CTA of phantom. *Chin J Med Imaging Technol (Chinese)*. 2018;34(7):1085-1089.
5. Wang Y, Chen B, Ren H. Contrast optimization imaging in neck CT angiography based on dual energy nonlinear image blending technology. *J Pract Radiol (Chinese)*. 2020;36(10):1659-1662.
 6. Lin ZY, Wang HH, Liu JX, et al. Application of dual-energy CT angiography with linear blending technique in peripancreatic angiography: optimal selection of weighting factor. *Radiol Practice (Chinese)*. 2017;32(8):851-855.
 7. Li Q, Tan H, Lv F. Molecular characterization of solitary pulmonary nodules in dual-energy CT nonlinear image fusion technology. *J Recept Signal Transduct Res*. 2022;42(1):95-99.
 8. Alobeidi H, Alshamari M, Widell J, et al. Minimizing contrast media dose in CT pulmonary angiography with high-pitch technique. *Br J Radiol*. 2020;93(1111):20190995.
 9. Meyer M, Haubenreisser H, Schabel C, et al. CT pulmonary angiography in patients with acute or chronic renal insufficiency: Evaluation of a low dose contrast material protocol. *Sci Rep*. 2018;8(1):1995.
 10. Kim KS, Lee JM, Kim SH, et al. Image fusion in dual energy computed tomography for detection of hypervascular liver hepatocellular carcinoma: phantom and preliminary studies. *Invest Radiol*. 2010;45(3):149-157.
 11. Cao R, Jiang Y, Lu J, et al. Evaluation of intracranial vascular status in patients with acute ischemic stroke by time maximum intensity projection CT angiography: A preliminary study. *Acad Radiol*. 2020;27(5):696-703.
 12. Schneeweiss S, Esser M, Thaiss W, et al. Improved CT-detection of acute bowel ischemia using frequency selective non-linear image blending. *Acta Radiol Open*. 2017;6(7):2058460117718224.
 13. Schwarz R, Bongers NM, Hinterleitner C, et al. Frequency-selective non-linear blending for the computed tomography diagnosis of acute gangrenous cholecystitis: Pilot retrospective evaluation. *Eur J Radiol Open*. 2018;5:114-120.
 14. Bongers MN, Bier G, Kloth C, et al. Improved delineation of pulmonary embolism and venous thrombosis through frequency selective nonlinear blending in computed tomography. *Invest Radiol*. 2017;52(4):240-244.

DOI 10.1007/s10330-021-0544-4

Cite this article as: Yi SQ, Zhou P, He YK, et al. The application study of dual-energy CT nonlinear blending technique in pulmonary angiography. *Oncol Transl Med*. 2023;9(1):-.